Journal of Power Sources 240 (2013) 42–49

Contents lists available at SciVerse ScienceDirect

Journal of Power Sources

journal homepage: www.elsevier.com/locate/jpowsour

Influence of current collector on capacitive behavior and cycling stability of Tiron doped polypyrrole electrodes

Kaiyuan Shi, Igor Zhitomirsky*

Department of Materials Science and Engineering, McMaster University, 1280 Main St. West, Hamilton, Ontario, Canada L8S 4L7

HIGHLIGHTS

- Polypyrrole electrodes for supercapacitors were prepared by electropolymerization.
- Tiron was used as an anionic dopant for deposition on Ni foils and plaques.
- The use of Tiron allowed the fabrication of adherent films.
- Ni plaque based electrodes allowed higher capacitance and good capacitance retention.

GRAPHICAL ABSTRACT

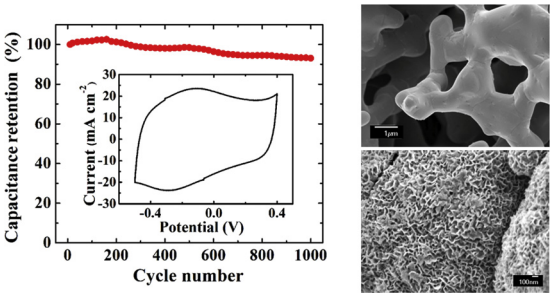

ARTICLE INFO

Article history:
Received 4 December 2012
Received in revised form
26 February 2013
Accepted 27 March 2013
Available online 11 April 2013

Keywords:
Supercapacitor
Electropolymerization
Polypyrrole
Stability
Retention
Capacitance

ABSTRACT

In this work we demonstrate the feasibility of electrodeposition of adherent polypyrrole (PPy) films on Ni substrates using Tiron as an anionic dopant. Compared to other aromatic sulfonate dopants, Tiron offers the advantages of higher charge to mass ratio and chelating properties, which are beneficial for the efficient charge transfer during electropolymerization and fabrication of adherent films. The use of Ni plaque current collectors allows higher capacitance and higher PPy loading compared to Ni foil current collectors. Moreover, the use of Ni plaques allows significant improvement in capacitance retention at high scan rates. The problem of poor cycling stability of PPy films on Ni foil current collectors is successfully addressed by the use of Ni plaques. The electron microscopy studies and impedance spectroscopy measurements during cycling provide an insight into the factors, controlling capacitance retention. The results indicate that for pure PPy electrodes the mass normalized specific capacitance of 339–451 F g^{-1} and area normalized specific capacitance of 0.4–0.95 F cm^{-2} can be achieved for material loadings of 0.84–2.80 mg cm^{-2}. The PPy electrodes formed on Ni plaque current collectors are promising for applications in electrochemical supercapacitors.

1. Introduction

The growing interest in application of polypyrrole (PPy) for electrodes of electrochemical supercapacitors (ES) is attributed to high specific capacitance and electrical conductivity, low cost and chemical stability of PPy [1,2]. Many investigations have been conducted with the objective to utilize high specific capacitance [2,3] of PPy in ES. The capacitive behavior of PPy with theoretical capacitance of 620 F g^{-1} results from redox reactions, which allow charge storage in the bulk of the electrode material. The specific capacitance of PPy is lower than that of other active materials for ES, such as MnO_2 [4,5]. However, the fabrication of MnO_2 electrodes requires the use of conductive additives (15–30%) and binders (5–10%) [6–9], which reduce the specific capacitance of the composite material. The use of conductive additives and binders can be

* Corresponding author. Tel.: +1 905 525 9140x23914.
E-mail address: zhitom@mcmaster.ca (I. Zhitomirsky).

0378-7753/$ – see front matter © 2013 Elsevier B.V. All rights reserved.
http://dx.doi.org/10.1016/j.jpowsour.2013.03.163

avoided in pure PPy electrodes due to high conductivity, binding and film forming properties of PPy.

Electropolymerization is an attractive method for the fabrication of PPy electrodes for ES. In this approach, anodic polymerization of PPy allows the pyrrole monomer, dissolved in a solvent, containing an anionic dopant, to be oxidized at the electrode surface by the applied anodic potential, forming a polymer film [2,10]. Many studies were focused on the development of advanced anionic dopants for PPy electropolymerization. Relatively high electrical conductivity and thermal stability of PPy films was achieved using aromatic anionic dopants [11–14]. It was shown that with the variation of the dopant anion, the conductivity of the PPy thin films can differ by three orders of magnitude [15]. The investigation of aromatic dopants, containing sulfonic anionic groups, showed that the conductivity of PPy films increased with increasing charge/mass ratio of the dopant molecules [12]. These studies generated significant interest in the use of 4,5-dihydroxy-1,3-benzenedisulfonic acid disodium salt (Tiron), which has higher charge/mass ratio, compared to that of toluenesulfonate, naphthalene sulfonate, naphthalene disulfonate and other aromatic sulfonate molecules used as anionic dopants for PPy electropolymerization [12]. The investigations of electropolymerization of PPy on Al alloy substrates in the presence of Tiron resulted in a discovery of its important properties [16]. It was shown that Tiron allowed the formation of continuous films and promoted charge transfer during electropolymerization. Compared to *p*-toluene sulfonic acid sodium salt [16], Tiron reduced deposition potential by 0.5 V, preventing Al alloy corrosion during electropolymerization. Moreover, the films prepared using Tiron as an anionic dopant and charge transfer mediator showed improved conductivity and adhesion. The use of Tiron allowed the formation of adherent PPy films on stainless steel substrates by electropolymerization from aqueous pyrrole solutions [17]. The films were investigated for application in ES [17]. These results also indicated that Tiron strongly adsorbed on the Al alloy and stainless steel surfaces [16,17]. It is in this regard that Tiron is a strong complexing agent [18–20], which belongs to the catechol family of aromatic materials. Recent investigations showed that materials from catechol family exhibit strong adhesion to various inorganic materials [21–24]. The chelating properties of Tiron and other catecholates are related to hydroxyl groups bonded to adjacent carbon atoms of the aromatic ring. The proposed chemisorption mechanism involved the deprotonation of the phenolic hydroxyl groups of the catechol and chelation of metal ions on the inorganic surface [21,22]. It is important to note that catecholate bonding facilitated charge transfer between inorganic and organic materials [25]. The strong adhesion of catecholates to various surfaces in the solutions of high ionic strength is especially attractive for the development of polymer film electrodes for electrochemical devices, containing aqueous electrolytes.

The goal of this investigation was the electropolymerization of PPy on Ni substrates, using Tiron as an anionic dopant, for the fabrication of electrodes of ES. The important finding was the possibility of electropolymerization of Tiron-doped PPy on commercial Ni plaque current collectors with high surface area, which allowed improved contact with active material. The results presented below indicated that high capacitance, good capacitance retention at high scan rates and good cycling stability can be achieved in pure PPy electrodes with relatively high materials loading. The analysis of the electrochemical impedance of PPy electrodes during cycling and corresponding SEM data provided an insight into the mechanism of capacitance decrease during cycling and paved a way for the fabrication of PPy electrodes with good cycling stability. The comparison of the experimental data for Ni foils and Ni plaque substrates showed that the use of Ni plaques offers benefits of significantly higher capacitance and materials loading, good capacitance retention at high charge–discharge rates and good cycling stability.

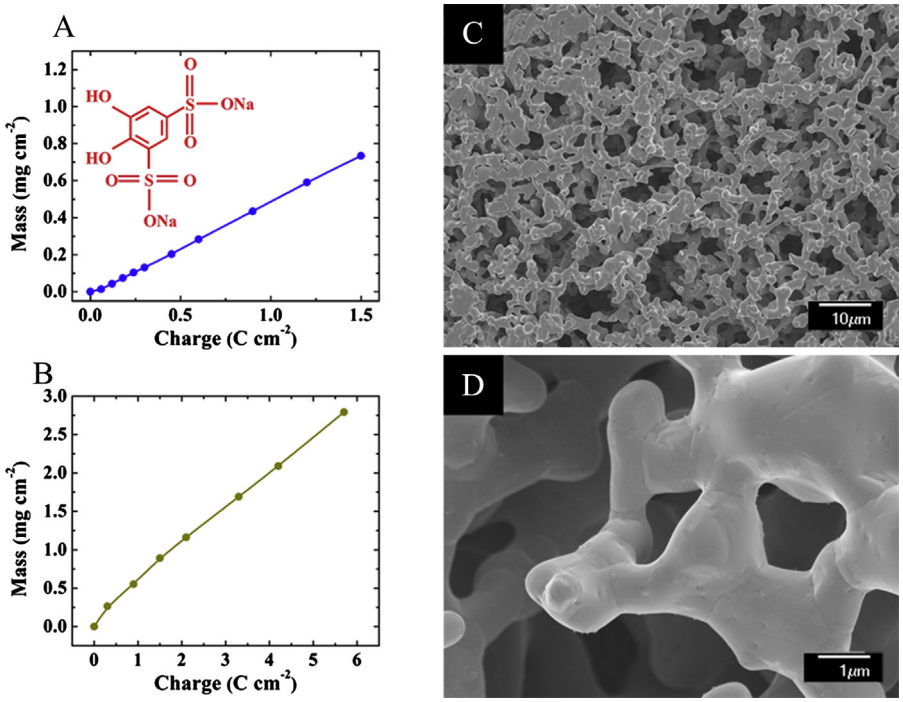

Fig. 1. (A, B) Deposit mass versus charge passed for deposition on (A) Ni foil (inset shows a chemical structure of Tiron dopant) and on (B) Ni plaque substrates and (C, D) SEM images of Ni plaques at different magnifications.

2. Experimental procedures

Pyrrole and 4,5-dihydroxy-1,3-benzenedisulfonic acid disodium salt (Tiron) were purchased from Sigma–Aldrich. Ni plaques with 80% porosity and pore size in the range of 1–10 μm were supplied by Vale company. The electrodeposition cell included a Ni foil or Ni plaque substrate and a Pt counter electrode. Electropolymerization was performed galvanostatically at a current density of 1 mA cm^{-2} from an aqueous 0.1 M pyrrole solution containing 0.005 M Tiron. All the deposition experiments were performed from freshly prepared solutions. After deposition, the working electrodes were rinsed with deionized water and then dried in air. The PPy deposits were investigated using a JEOL JSM-7000F scanning electron microscope (SEM). The measurements of film adhesion were performed according to the ASTM D3359 standard. According to the standard, a lattice pattern was made with cuts 1 mm apart in X and Y directions in the film to the substrate. A pressure-sensitive tape was applied over the lattice pattern and then removed. The adhesion was evaluated by comparison of the lattice pattern after tape removal with a classification table presented in the standard.

Electrochemical studies were performed using a potentiostat (PARSTAT 2273, Princeton Applied Research). Surface area of the working electrode was 1 cm^2. The counter electrode was a platinum gauze, and the reference electrode was a standard calomel electrode (SCE). Capacitive behavior and electrochemical impedance of the films were investigated in 0.5 M Na_2SO_4 aqueous solutions. Cyclic voltammetry (CV) studies were performed within a potential range of −0.5 to +0.4 V versus SCE at scan rates of 2–100 mV s^{-1}. The total capacitance $C = Q/\Delta V$ was calculated using half the integrated area of the CV curve to obtain the charge (Q), and subsequently dividing the charge by the width of the potential window (ΔV). The mass-normalized specific capacitance $C_m = C/m$ (m-sample mass) and area-normalized specific capacitance $C_s = C/S$ (S-geometric sample area), calculated from the CV data, were investigated versus mass loading, scan rate and cycle number. In the experimental data presented below, the capacitance retention $R_r = C(100)/C(2)$ is the ratio of $C(100)$ measured at a scan rate of 100 mV s^{-1} to the $C(2)$ measured at a scan rate of 2 mV s^{-1}. The capacitance retention $R_N = C(50)_N/C(50)_1$ is the ratio of $C(50)_N$ for cycle number N to the $C(50)_1$ for the first cycle, measured at a scan rate of 50 mV s^{-1}.

The alternating current (AC) measurements of complex impedance $Z^* = Z' - iZ''$ were conducted in the frequency range of 10 mHz–100 kHz and the amplitude of AC signal of 5 mV. The impedance data was also analyzed using the method, described in Ref. [26]. In this method, the complex capacitance $C^* = C' - iC''$ was calculated from the impedance data as $C' = Z''/\omega|Z|^2$ and $C'' = Z'/\omega|Z|^2$, where $\omega = 2\pi f$, f – frequency.

3. Results and discussion

Fig. 1(inset) shows a chemical structure of Tiron. The anionic properties of Tiron are related to SO_3^- groups. Similar to other materials from the catechol family, Tiron has two OH groups, bonded to adjacent carbon atoms of the aromatic ring. Such OH groups are assumed to form bidentate bonding of catechol with metal atoms on the material surface [27]. The chelation mechanism involves deprotonation of OH groups and complexation of metal atoms. Due to such structure and chelating properties, various catechols are important and versatile building blocks of synthetic adhesives and coatings [27,28].

PPy films were obtained on Ni foil substrates by electropolymerization from pyrrole solutions containing Tiron. Fig. 1A shows nearly linear dependence of the deposit mass versus charge passed. Such dependence indicated continuous film growth without induction time. It should be noted that induction time [29–31] was observed in experiments performed using other anionic dopants, and was related to substrate dissolution and

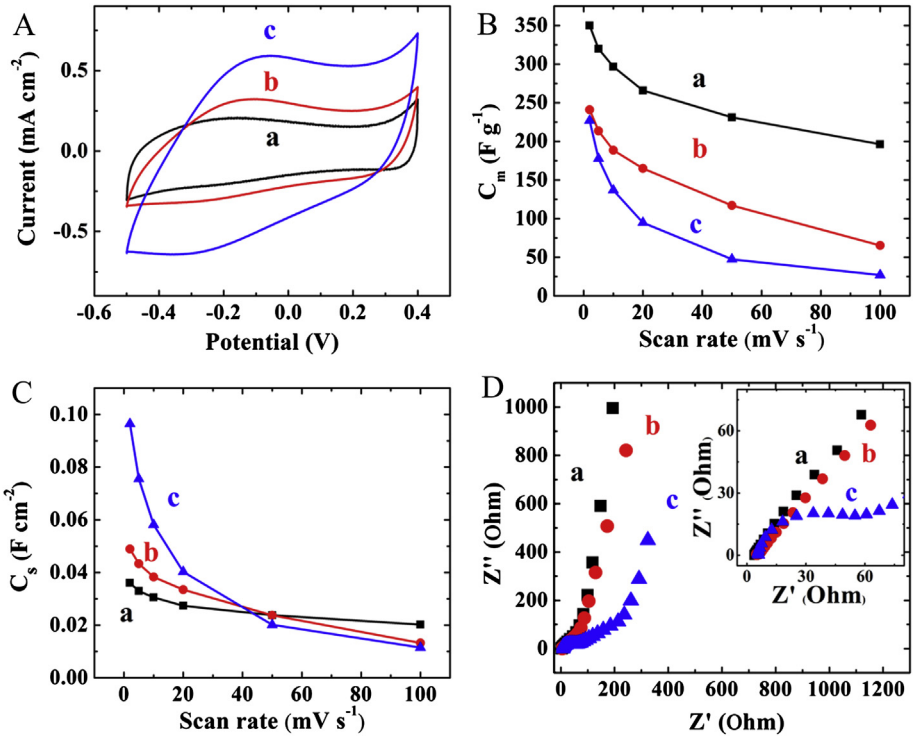

Fig. 2. (A) CVs at a scan rate of 5 mV s^{-1}, (B) C_m and (C) C_s obtained from the CV data versus scan rate and (D) Nyquist plot of Z^* (inset shows high frequency range) for PPy deposits on Ni foil with PPy mass of (a) 0.10, (b) 0.20 and (c) 0.42 mg cm^{-2}.

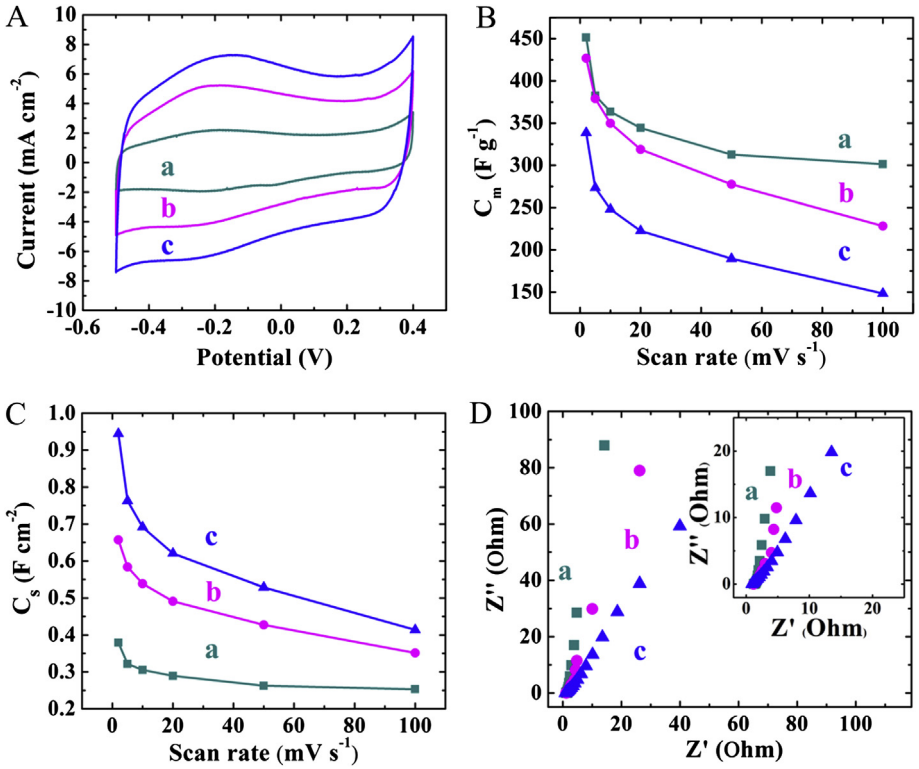

Fig. 3. (A) CVs at a scan rate of 5 mV s^{-1}, (B) C_m and (C) C_s obtained from the CV data versus scan rate and (D) Nyquist plot of Z^* (inset shows high frequency range) for PPy deposits on Ni plaque with PPy mass of (a) 0.84, (b) 1.54 and (c) 2.80 mg cm^{-2}.

passivation. Thin films with mass below 0.4 mg cm^{-2} were well adherent to Ni foil substrates. The measurements of film adhesion according to the ASTM D3359 standard showed that adhesion strength corresponded to the 4B classification. However, adhesion decreased with increasing film mass, especially for film mass above 1 mg cm^{-2}. In order to increase the mass of PPy deposits, electropolymerization was performed on commercial Ni plaque current collectors, designed for high power battery applications [32]. The deposits mass increased with increasing charge passed, showing nearly linear dependence (Fig. 1B) in the range of 0–3 mg cm^{-2}. Relatively high mass of PPy deposits was achieved because of porous microstructure of the Ni plaques (Fig. 1C). The pore size of Ni-plaques was in the range of 1–10 μm (Fig. 1C and D), in agreement with the information provided by the manufacturer. Such pores were impregnated with PPy during electropolymerization. The deposition yield for plaques was slightly higher compared to that for foils at the same charge passed. It is important to note that pyrrole monomer has no charge and electropolymerization kinetics is controlled by diffusion. 3-D porous plaques with high surface area provided higher deposition efficiency due to better pyrrole access to their surface.

The initial open circuit potential of the PPy coated Ni substrates was −0.01 V versus SCE. The PPy films formed on Ni substrates showed capacitive behavior in the voltage window of −0.5 to +0.4 V versus SCE. Fig. 2A shows typical CVs for films of different mass on Ni foil substrates. Thin films showed nearly box shape CVs, however significant deviation from the ideal box shape CV was observed when film mass was above 0.3 mg cm^{-2}. Measurements of C_m and C_s at different conditions are important for understanding electrochemical behavior of PPy electrodes and optimizing their performance. The C_m calculated from the CV data for 0.1 mg cm^{-2} film at a scan rate of 2 mV s^{-1} was found to be 350 F g^{-1}. The increase in scan rate and mass loading resulted in decreasing C_m (Fig. 2B). The C_m of the films deposited on Ni substrates was higher, compared to C_m of films formed on stainless steel [17]. However, recent studies [33] showed that high C_m values of electrode materials do not necessarily indicate good capacitive behavior. It was shown that reporting gravimetric characteristics (such as C_m) alone cannot provide realistic picture of material performance, especially at high material loadings. Therefore, C_s data for the films were presented in Fig. 2C and analyzed. The increase in film mass resulted in increasing C_s at low scan rates. In contrast, at high scan

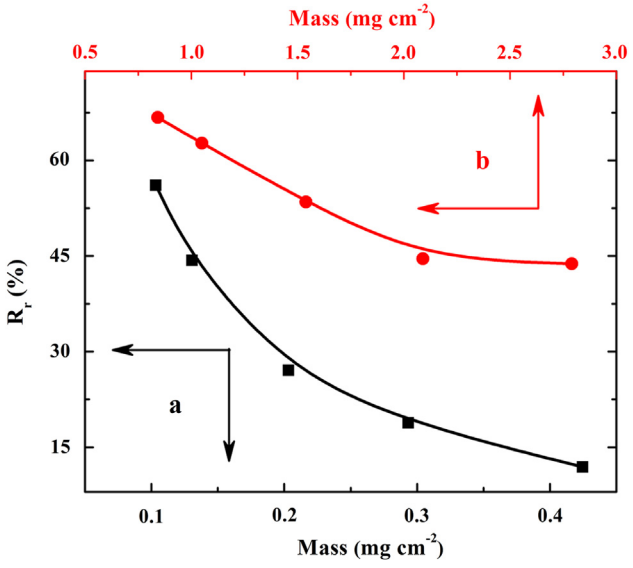

Fig. 4. R_r versus mass of PPy deposits on (a) Ni foil and (b) Ni plaque substrates.

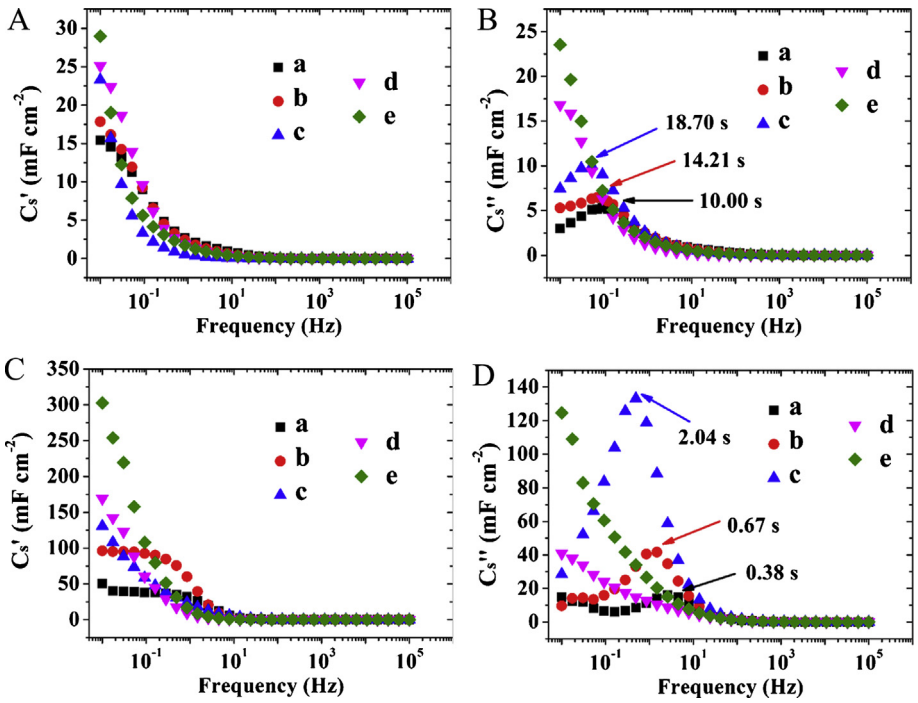

Fig. 5. C_s^* obtained from impedance data versus frequency for PPy deposits on (A, B) Ni foil with PPy mass of (a) 0.10, (b) 0.13, (c) 0.20, (e) 0.29 and (f) 0.42 mg cm^{-2} and (C, D) Ni plaque with PPy mass of (a) 0.84, (b) 1.16, (c) 1.54, (e) 2.09 and (f) 2.80 mg cm^{-2}.

rates the C_S decreased with increasing film mass. It is suggested that diffusion limitations at high scan rates resulted in poor electrolyte access to the bulk of thick PPy films. It is in this regard that corresponding impedance data, presented in a Nyquist plot (Fig. 2D), showed the increase in real part of impedance Z' with increasing film mass. Therefore, bulk PPy material behaved as a capacitor with low capacitance, connected in series with a surface layer with a high capacitance, and reduced total C_S of thick PPy films.

The comparison of experimental data for Ni foil (Fig. 2) and Ni plaque (Fig. 3) based electrodes showed that significant improvement in capacitive behavior at higher materials loading can be achieved using Ni plaque current collectors. The box shape CVs

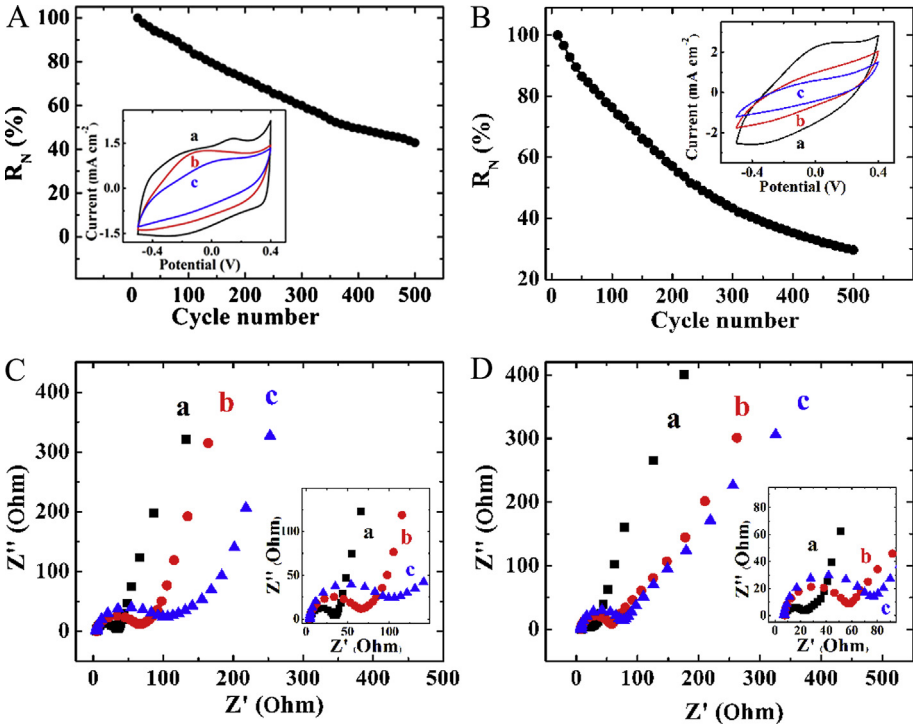

Fig. 6. (A, B) R_N versus cycle number (insets show CVs for (a) 10th (b) 250th and (c) 500th cycle) and (C, D) Nyquist plots of Z^* obtained after the corresponding cycles (insets show high frequency range) for (A, C) 0.15 and (B, D) 0.31 mg cm^{-2} deposits on Ni foil.

were observed for materials loadings of 0.84–2.80 mg cm^{-2} (Fig. 3A). In contrast, the films on Ni foil substrates with similar material loadings showed poor adhesion and peeled off the substrates during testing. The C_m values calculated from the CVs at different scan rates showed remarkable improvement in capacitive behavior (Fig. 3B). The C_m at 2 mV s^{-1} for the Ni plaque based PPy electrodes with material loading of 0.42 and 0.84 mg cm^{-2} was 470 and 451 F g^{-1}, respectively. The C_m at 2 mV s^{-1} for 0.42 and 0.84 PPy films on Ni foil was only 227 and 198 F g^{-1}, respectively. As expected, the C_m decreased with increasing PPy mass (Fig. 3B). However, the analysis of corresponding C_s data (Fig. 3C) showed a different behavior, compared to the C_s data for thin film samples (Fig. 2C). The increase in PPy mass resulted in increasing C_s not only at low scan rates, but also at high scan rates (Fig. 3C). This is in contrast to the data for thin film samples formed on Ni foils (Fig. 2C), which showed decreasing C_s with increasing film mass at high scan rates. The impedance measurements showed that real part of impedance Z' increased with increasing mass of the electrode (Fig. 3D). However, the Ni plaques based PPy electrodes showed significantly lower Z' values, compared to the Ni foil based electrodes of smaller mass (Fig. 2D). The lower Z'' values of Ni plaque based PPy electrodes indicated higher capacitance.

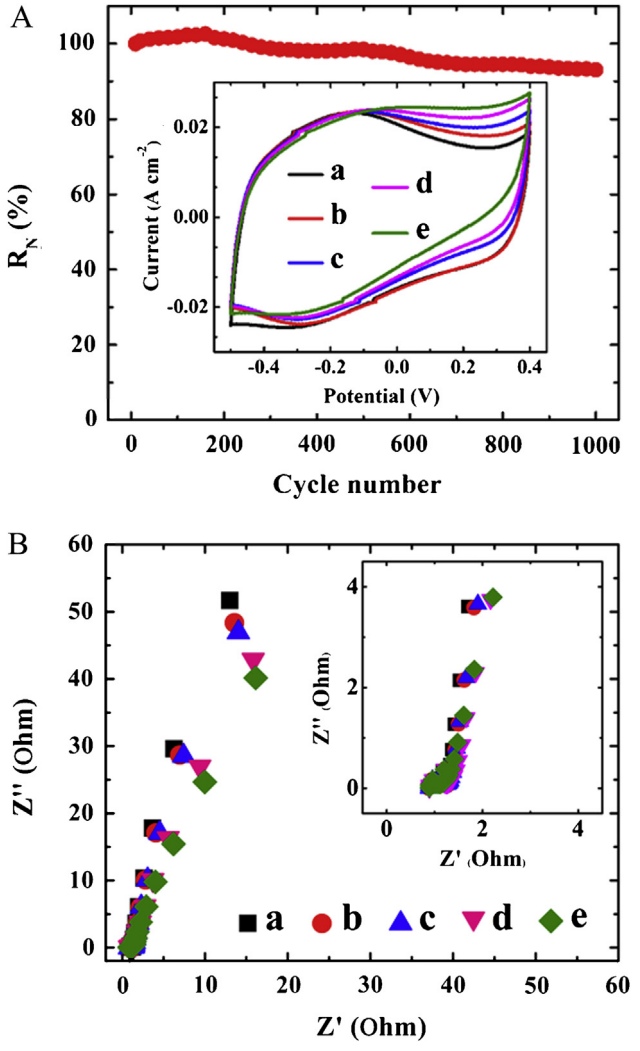

Fig. 7. (A) R_N versus cycle number (inset shows CVs for (a) 10th (b) 150th, (c) 500th, (d) 750th and (e) 1000th cycle) and (B) Nyquist plots of Z^* obtained after the corresponding cycles (inset shows high frequency range) for 1.10 mg cm^{-2} PPy deposit on a Ni plaque.

The experimental data presented in Fig. 3B and C indicated that the increase in PPy mass in the range of 0.84–2.80 mg cm^{-2} resulted in C_m decrease in the range of 451–339 F g^{-1} and corresponding C_s increase in the range of 0.4–0.95 F cm^{-2} at a scan rate of 2 mV s^{-1}. According to the literature, PPy electrodes with mass loading of 0.66 mg cm^{-2} prepared on stainless steel foil [34] and PPy electrodes with mass loading of 1 mg cm^{-2} on Ni foam [35] current collectors showed C_m of 110 and 310 F g^{-1} and C_s of 0.07 and 0.38 F cm^{-2}, respectively. Therefore, the use of Tiron as an anionic dopant for PPy and Ni plaque current collectors offers benefits of relatively high capacitance at higher materials loadings.

Fig. 4 compares capacitance retention R_r for thin PPy films deposited on Ni foils and for Ni-plaques based PPy electrodes. The increase in film mass from 0.10 to 0.42 mg cm^{-2} resulted in R_r reduction from 56 to 10%. The Ni plaque based PPy electrodes showed significantly higher R_r values even at higher materials loadings. The increase in mass loading from 0.84 to 2.80 mg cm^{-2} resulted in R_r decrease in the range from 68 to 43%. The decrease in R_r was attributed to diffusion limitations of electrolyte in pores of PPy electrodes. The use of porous Ni plaques allowed better electrolyte access to active material even at significantly higher materials loadings. These results are in agreement with C^* data obtained from impedance measurements by the method described above.

Fig. 5A indicates that C_s' of thin films on Ni foils decreased with increasing frequency. The corresponding C_s'' curves showed maxima, which shifted to lower frequencies with increasing film mass. Such dependencies indicated relaxation type of dispersion,

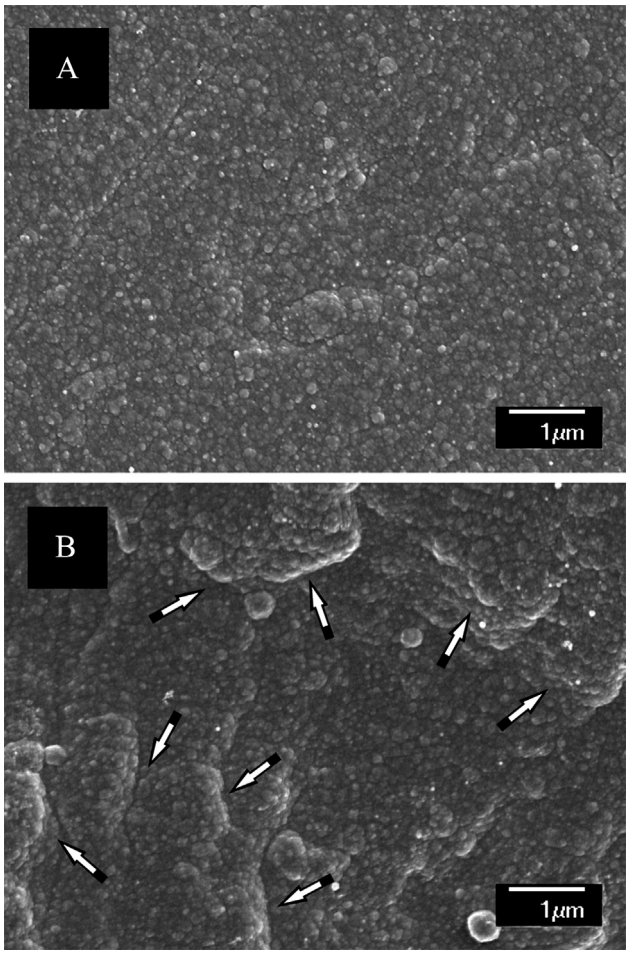

Fig. 8. SEM images of 0.15 mg cm^{-2} PPy deposit on a Ni foil: (A) as prepared and (B) after 500 cycles, arrows show areas of deposit swelling.

attributed to slow diffusion of electrolyte in pores of active material. The relaxation times $\tau = 1/f_m$ were calculated from the relaxation frequencies f_m, corresponding to the C_s'' maxima. The τ values of 10.00, 14.21, and 18.70 s were obtained for film mass of 0.10, 0.13, and 0.20 mg cm^{-2}, respectively (Fig. 5B). The Ni plaque based PPy electrodes with materials loading of 0.84–2.80 mg cm^{-2} showed remarkably higher C_s' values (Fig. 5C). Another advantage of such electrodes is related to higher relaxation frequencies. The frequency dependence of C_s' for 0.84 mg cm^{-2} electrode showed a plateau below ~1 Hz, then the C_s' decreased at higher frequencies. The increase in PPy electrode mass resulted in the relaxation type dispersion at lower frequencies. The PPy electrode with mass of 1.16 mg cm^{-2} showed a plateau in the frequency dependence below ~0.5 Hz and then C_s' decreased. The corresponding C_s'' dependencies (Fig. 5D) showed relaxation maxima, which shifted to lower frequencies with increasing electrode mass. The relaxation times $\tau = 1/f_m$ were found to be 0.38, 0.67 and 2.04 s for PPy electrode mass of 0.84, 1.16 and 1.54 mg cm^{-2}. Therefore, the results of C^* analysis indicated that Ni plaque based electrodes allowed higher capacitance, better capacitance retention at higher frequencies and higher electrode mass.

Fig. 6 shows the influence of cycling on electrochemical behavior of PPy films on Ni foil substrates. The capacitance, calculated from the CV data decreased with increasing cycle number (Fig. 6A). The increase in film mass resulted in reduced capacitance retention (Fig. 6B). The corresponding CV data showed continuous reduction in CV area (Fig. 6A and B insets) with increasing cycle number. The R_{500} for 0.31 mg cm^{-2} electrode was only 29.6%. Due to poor cycling stability of the thin film samples the testing was limited to 500 cycles. Fig. 6C and D shows Nyquist plots for impedance measured after 10, 250 and 500 cycles for the same samples. The increase in real part of impedance Z' was observed, which correlated with capacitance measurements for the corresponding cycles. The use of Ni plaque based electrodes allowed improved cycling stability even at higher material loadings.

Fig. 7 shows R_N as a function of cycle number for 1.10 mg cm^{-2} PPy electrode. Testing results indicated a small increase in R_N during the first 150 cycles, then R_N decreased. The R_{500} and R_{1000} values were found to be 97.49% and 93.09%, respectively. The analysis of CVs for 10th, 150th, 500th, 750th and 1000th cycles (Fig. 7A inset) revealed some changes in CV shape, more evident in the potential range of 0–0.4 V. Such change can be attributed to increased resistance. Indeed, impedance spectroscopy data obtained after corresponding cycles (Fig. 7B) showed increase in real part of impedance Z' with increasing cycle number. However, the changes in Z' for Ni plaque based PPy electrodes (Fig. 7B) were relatively small, compared to thin film electrodes on Ni foils (Fig. 6C and D).

SEM data provided additional information related to cycling behavior of the PPy electrodes. Fig. 8A shows a SEM image of a PPy film on a Ni foil substrate. The film was relatively dense. The electrolyte diffusion in such films presented difficulties. As a result, C_m and C_s decreased with increasing scan rate (Fig. 2B and C). Electrochemical cycling resulted in film swelling (Fig. 8B), which increased with increasing cycle number. The film partially detached from the substrates after 1000 cycles. The film swelling and partial detachment from the substrate resulted in poor electrical contact of the film and Ni foil current collectors. Therefore, SEM observations can explain the increase in real part of impedance Z' during cycling (Fig. 6C and D) and poor cycling stability (Fig. 6A and B).

Fig. 9 shows SEM images of a PPy electrode formed on a Ni plaque current collector. The comparison of the SEM images of as-received porous Ni plaques (Fig. 1C and D) and the plaques after electropolymerization (Fig. 9) confirmed the formation of PPy. The SEM images at low magnification showed that PPy surface (Fig. 9A) was relatively rough and exhibited cracks. The size of PPy particles was in the range of 1–5 μm. It is suggested that the PPy microstructure is influenced by the microstructure of porous current collector. Large pores in the plaques below the surface of the PPy layer can promote cracking in the surface layer. The SEM image of as-deposited PPy at high magnification showed relatively rough and dense surface (Fig. 9C). Turning again to the SEM image of a Ni plaque (Fig. 1D) it is suggested that PPy deposition on the porous 3-D network formed by sintered Ni particles, resulted in rough surface of the PPy deposit. Cycling resulted in enhanced cracking of the surface layers and

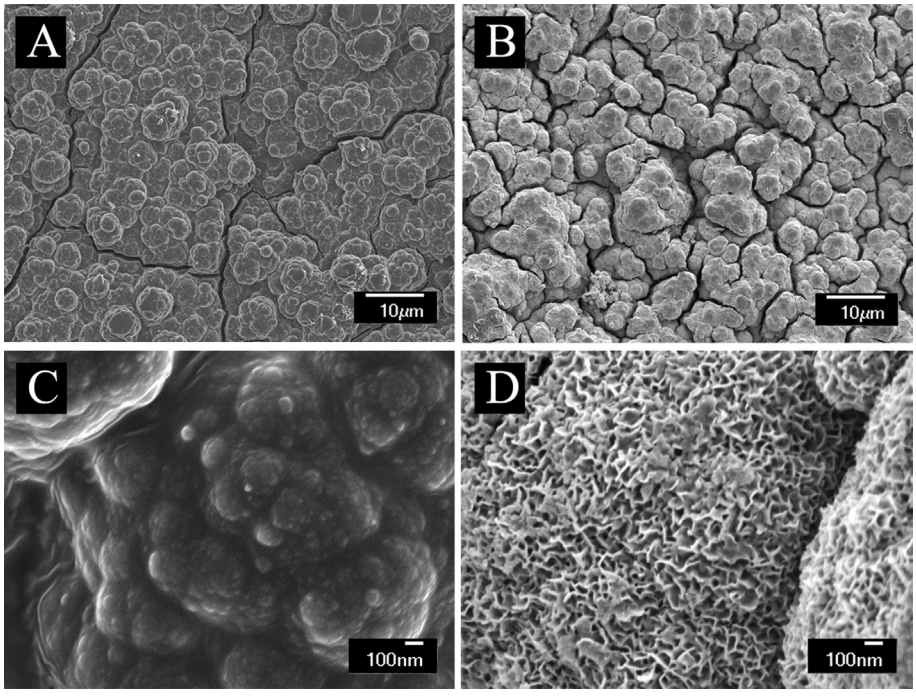

Fig. 9. (A–D) SEM images of impregnated Ni plaques at different magnifications: (A, C) before cycling and (B, D) after 1000 cycles.

enhanced macroporosity (Fig. 9B). Such changes can result from PPy swelling in the surface layer during cycling. The SEM image of the cycled sample at high magnification (Fig. 9D) revealed microporosity with pore size of about 50 nm. The development of microporosity and cracking in the surface layers can result in improved electrolyte access to the bulk material. Such morphology changes can explain capacitance increase during the first 150 cycles (Fig. 7A). However, similar to thin PPy films, the swelling of the surface layers of PPy impregnated plaques can result in reduced capacitance (Fig. 7A). However, it is suggested that porous Ni network of the plaques limited the swelling of bulk PPy material, which resulted in improved capacitance retention during cycling.

Compared to Ni foil current collectors, the use of Ni plaques allowed increased C_m and C_s at high materials loadings, improved capacitance retention at high scan rates and good cycling stability. It is important to note that in many recent investigations the improved capacitive behavior was achieved by the development of PPy based composites, containing various additives, such as carbon nanotubes [3], MnO_2 [36] and graphene [37,38]. However, in this investigation we obtained higher capacitance and good capacitance retention of pure PPy electrodes with higher materials loadings, compared to PPy based composites [3,36–38]. This was achieved using Tiron as an anionic dopant and Ni plaque current collectors. Eliminating the use of additives offers important processing advantages, because the problems related to additive preparation, dispersion, electrodeposition and control of deposit composition can be avoided.

4. Conclusions

PPy was deposited by electropolymerization method on Ni foil and Ni plaque current collectors for application in ES. The use of Tiron, as an anionic dopant with chelating properties, allowed electrodeposition of adherent PPy films on the Ni foil substrates. The results indicate that the C_m of 339–451 F g^{-1} and C_s of 0.4–0.95 F cm^{-2} can be achieved for pure PPy electrodes for material loadings of 0.84–2.80 mg cm^{-2}. Compared to Ni foil current collectors, the use of Ni plaques allowed increased capacitance at high materials loadings, improved capacitance retention at high scan rates and good cycling stability. Ni plaques limited PPy swelling during cycling and allowed improved cycling stability. Improved capacitive behavior of PPy electrodes was achieved without additives, such as CNT, graphene or MnO_2. Eliminating the use of additives offers processing advantages. The PPy electrodes obtained using Ni plaque current collectors are promising for applications in ES.

Acknowledgment

The authors gratefully acknowledge the financial support of the Natural Sciences and Engineering Research Council of Canada.

References

[1] P. Simon, Y. Gogotsi, Nature Materials 7 (2008) 845–854.
[2] G.A. Snook, P. Kao, A.S. Best, Journal of Power Sources 196 (2011) 1–12.
[3] X. Li, I. Zhitomirsky, Journal of Power Sources 221 (2013) 49–56.
[4] A. Sumboja, U.M. Tefashe, G. Wittstock, P.S. Lee, Journal of Power Sources 207 (2012) 205–211.
[5] D. Yan, Z. Guo, G. Zhu, Z. Yu, H. Xu, A. Yu, Journal of Power Sources 199 (2012) 409–412.
[6] T. Brousse, P.-L. Taberna, O. Crosnier, R. Dugas, P. Guillemet, Y. Scudeller, Y. Zhou, F.d.r. Favier, D. Belanger, P. Simon, Journal of Power Sources 173 (2007) 633–641.
[7] W. Tang, Y.Y. Hou, X.J. Wang, Y. Bai, Y.S. Zhu, H. Sun, Y.B. Yue, Y.P. Wu, K. Zhu, R. Holze, Journal of Power Sources 197 (2012) 330–333.
[8] R. Jiang, T. Huang, Y. Tang, J. Liu, L. Xue, J. Zhuang, A. Yu, Electrochimica Acta 54 (2009) 7173–7179.
[9] R.N. Reddy, R.G. Reddy, Journal of Power Sources 124 (2003) 330–337.
[10] D.P. Dubal, S.H. Lee, J.G. Kim, W.B. Kim, C.D. Lokhande, Journal of Materials Chemistry 22 (2012) 3044–3052.
[11] I. Carrillo, E.S. De La Blanca, M.I. Redondo, M.V. Garcia, M.J. Gonzalez-Tejera, J.L.G. Fierro, E. Enciso, Synthetic Metals 162 (2012) 136–142.
[12] G.R. Mitchell, F.J. Davis, C.H. Legge, Synthetic Metals 26 (1988) 247–257.
[13] J. Tamm, T. Raudsepp, M. Marandi, T. Tamm, Synthetic Metals 157 (2007) 66–73.
[14] T. Raudsepp, M. Marandi, T. Tamm, V. Sammelselg, J. Tamm, Electrochimica Acta 53 (2008) 3828–3835.
[15] P.-C. Wang, J.-Y. Yu, Reactive and Functional Polymers 72 (2012) 311–316.
[16] D.E. Tallman, C. Vang, G.G. Wallace, G.P. Bierwagen, Journal of The Electrochemical Society 149 (2002) C173–C179.
[17] C. Shi, I. Zhitomirsky, Surface Engineering 27 (2011) 655–661.
[18] L. Jiang, L. Gao, Y. Liu, Colloids and Surfaces A 211 (2002) 165–172.
[19] C. Kawaguti, C. Santilli, S. Pulcinelli, Journal of Non-Crystalline Solids 354 (2008) 4790–4794.
[20] M. Kass, A. Ivaska, Talanta 58 (2002) 1131–1137.
[21] H. Lee, S.M. Dellatore, W.M. Miller, P.B. Messersmith, Science 318 (2007) 426–430.
[22] J.H. Waite, Nature Materials 7 (2008) 8–9.
[23] Y. Wang, I. Zhitomirsky, Journal of Colloid and Interface Science 380 (2012) 8–15.
[24] Y. Sun, M.S. Ata, I. Zhitomirsky, Journal of Colloid and Interface Science 369 (2012) 395–401.
[25] G.-L. Wang, J.-J. Xu, H.-Y. Chen, Biosensors and Bioelectronics 24 (2009) 2494–2498.
[26] P. Taberna, P. Simon, J.F. Fauvarque, Journal of The Electrochemical Society 150 (2003) A292–A300.
[27] E. Faure, C. Falentin-Daudre, C. Jerome, J. Lyskawa, D. Fournier, P. Woisel, C. Detrembleur, Progress in Polymer Science (2012).
[28] B.P. Lee, P.B. Messersmith, J.N. Israelachvili, J.H. Waite, Annual Review of Materials Research 41 (2011) 99–132.
[29] W.J. Hamer, L. Koene, J.H.W. De Wit, Materials and Corrosion 55 (2004) 653–658.
[30] W. Su, J.O. Iroh, Journal of Applied Polymer Science 65 (1997) 417–424.
[31] A. De Bruyne, J.L. Delplancke, R. Winand, Surface and Coatings Technology 99 (1998) 118–124.
[32] A.Y. Zaitsev, D.S. Wilkinson, G.C. Weatherly, T.F. Stephenson, Journal of Power Sources 123 (2003) 253–260.
[33] Y. Gogotsi, P. Simon, Science 334 (2011) 917–918.
[34] C. Shi, I. Zhitomirsky, Nanoscale Research Letters 5 (2010) 518–523.
[35] Z.H. Dong, Y.L. Wei, W. Shi, G.A. Zhang, Materials Chemistry and Physics 131 (2011) 529–534.
[36] R.K. Sharma, A. Karakoti, S. Seal, L. Zhai, Journal of Power Sources 195 (2010) 1256–1262.
[37] H.-H. Chang, C.-K. Chang, Y.-C. Tsai, C.-S. Liao, Carbon 50 (2012) 2331–2336.
[38] P. Mini, A. Balakrishnan, S.V. Nair, K. Subramanian, Chemical Communications 47 (2011) 5753–5755.